Reverse phase protein array for the quantification and validation of protein biomarkers of beef qualities: The case of meat color from Charolais breed

Mohammed Gagaoua, Muriel Bonnet, Leanne de Koning, Brigitte Picard

Meat Science 145 (2018) 308–319

Contents lists available at ScienceDirect

Meat Science

journal homepage: www.elsevier.com/locate/meatsci

Reverse Phase Protein array for the quantification and validation of protein biomarkers of beef qualities: The case of meat color from Charolais breed

Mohammed Gagaoua[a,*], Muriel Bonnet[a], Leanne De Koning[b], Brigitte Picard[a]

[a] INRA, Université Clermont Auvergne, VetAgro Sup, UMR Herbivores, Saint-Genès-Champanelle F-63122, France
[b] Institut Curie centre de recherche, Université de recherche PSL Plateforme RPPA, 26 rue de l'UlM, Paris 75248, France

ARTICLE INFO

Keywords:
Biomarkers
RPPA
Meat color
Young bulls
Multivariate analyses
Mechanisms

ABSTRACT

Reverse Phase Protein Arrays (RPPA) were applied for the quantification and validation of protein biomarkers of beef qualities on *M. longissimus thoracis* sampled early *post-mortem* from young Charolais bulls. pHu was related to six proteins, three of which are glycolytic enzymes (ENO1, ENO3 and TPI1), while others belong to structural (TTN and α-actin) and proteolytic (μ-calpain) pathways. For color traits, several correlations were found, interestingly with structural proteins. The relationships were in some cases trait-dependent. To understand the mechanisms and explore animal variability, color data were categorized into three classes. α-actin and TTN allowed efficient separation of the classes and were strongly related with all color traits. Biomarkers belonging to heat stress and metabolism pathways were also involved. Two identified proteins, namely Four and a half LIM domains 1 (FHL1) and Tripartite motif-containing 72 (TRIM72), were for the first time related to beef color. Overall, these relationships could be used to develop muscle-specific processing strategies to improve beef color stability.

1. Introduction

Over the last decade, "Omics" – genomics, transcriptomics, proteomics and metabolomics – technologies are a novelty in food sciences and were successfully implemented to address meat quality issues (for review see (Picard & Gagaoua, 2017; Picard, Gagaoua, & Hollung, 2017). These powerful techniques were also extensively used to elucidate the biological basis/mechanisms for phenotypic variation in meat quality traits. Proteomics notably, which corresponds to the large-scale study of the proteome of a tissue at a given moment and condition, was applied in the field of meat quality with several objectives (for review see (Almeida et al., 2015; Picard et al., 2017; Picard & Gagaoua, 2017)). For example, proteomics was used to study meat tenderness variability (Morzel, Terlouw, Chambon, Micol, & Picard, 2008), to investigate technological meat quality traits likely water holding capacity, drip loss and pH (Di Luca, Hamill, Mullen, Slavov, & Elia, 2016) and also to study meat color stability and development (Hwang, Park, Kim, Cho, & Lee, 2005). The use of proteomic tools (two-dimensional electrophoresis and mass spectrometry) to study the muscle-specificity in beef color stability is recent and was first applied by (Joseph, Suman, Rentfrow, Li, & Beach, 2012). Later on, several studies on cattle meat were reported using high-throughput technologies, such as Dot-Blot (Gagaoua et al., 2015; Gagaoua, Couvreur, Le Bec, Aminot, & Picard, 2017) and label free mass spectrometry strategies (Yu et al., 2017) to identify proteins that would be linked with meat color parameters. These studies highlighted that several biological pathways contribute to the conversion of muscle into meat processes including meat color development. These pathways included heat shock, metabolic (glycolytic and oxidative), structural, oxidative stress, apoptotic, transport, signaling and proteolytic proteins (Picard et al., 2017). However, most of the proteomic studies failed to validate the identified proteins. The few investigations undertaken on beef or pork were conducted by our group and showed that certain proteins might be used as biomarkers to manage meat color through the first regression/prediction equations (Gagaoua, Couvreur, Le Bec, et al., 2017; Gagaoua, Terlouw, Micol, et al., 2015; Kwasiborski, Rocha, & Terlouw, 2009). We have also very recently suggested using certain biomarkers to classify beef cuts sampled early *post-mortem* (*p-m*) according to muscle/breed and their forthcoming color (Gagaoua, Terlouw, & Picard, 2017).

In this study, we report the use of Reverse Phase Protein Array (RPPA), a quantitative microformat Dot-Blot approach, for the quantification and then validation of protein biomarkers related to meat quality. In recent years, RPPA has emerged as a powerful high-throughput approach for targeted proteomics (Paweletz et al., 2001). As a major advantage, RPPA allows assessment of target protein abundance quantitatively in large sample sets while requiring only a very

* Corresponding author.
E-mail addresses: mohammed.gagaoua@inra.fr, gmber2001@yahoo.fr (M. Gagaoua).

https://doi.org/10.1016/j.meatsci.2018.06.039
Received 18 October 2017; Received in revised form 26 June 2018; Accepted 26 June 2018
Available online 05 July 2018
0309-1740/

low amount of biological sample. This makes this methodology very attractive for the analysis of meat and biomarker discovery/validation without excessive carcass depreciation (Gagaoua, Bonnet, Ellies-Oury, De Koning, & Picard, 2018). Despite recent studies, knowledge of large-scale proteomics analysis for understanding meat color is still lacking and techniques such as RPPA are sought and widely welcomed in the field of meat science for better understanding of the unknowns. Thus, the first objective of the present study was to help produce and validate a list of biomarkers, which may explain and predict meat color development or be used in the selection of beef cattle to produce stable meat color. For that, 29 proteins were quantified by RPPA in *Longissimus thoracis* muscle of young Charolais bulls sampled early *p-m*. Second, this study aimed to investigate the associations between the 29 proteins and pH and meat color coordinates, in order to seek understanding of the biological mechanisms potentially underlying muscle to meat conversion and hence those of meat color development in Charolais beef.

2. Materials and methods

2.1. Animals, handling and slaughtering

A total of 43 young Charolais bulls averaging 530 days of age were used. These animals constituted the dataset from the study of (Mialon et al., 2015) conducted in two INRA France experimental units: INRA-UE232 (Bourges) for animal rearing and handling and INRA-UE1414 Herbipôle (Theix) for lairage and slaughtering. These animals were all fattened for a minimum of 228 days with a high-concentrate diet composed of a concentrate mixture and barley straw fed *ad libitum* (Gagaoua, Bonnet, Ellies-Oury, et al., 2018). Before slaughter, all animals were food deprived for 24 h to limit the risk of carcass contamination by microbes in the digestive tract during evisceration, but had free access to water. At a live weight around 732 ± 65 kg, the animals were all slaughtered in the same conditions at the experimental slaughterhouse of INRA research center (Theix), stunned using captive-bolt pistol prior to exsanguination and dressed according to standard commercial practice. Slaughtering was performed in compliance with French welfare regulations and respecting EU regulations (Council Regulation (EC) No. 1099/2009).

2.2. Muscle sampling

The carcasses were processed by removal of the head, tail, feet, and abdominal and thoracic viscera. They were not electrically stimulated. Immediately after slaughter (at ~45 min *p-m*), muscle samples from *Longissimus thoracis* (LT, mixed fast oxido-glycolytic muscle) were excised from the center of the 6th rib located at the right side of each carcass as illustrated in (Gagaoua, Picard, & Monteils, 2018). The epimysium was carefully dissected and aliquots were subsequently frozen in liquid nitrogen and kept at −80 °C until protein extraction and RPPA analysis. Carcasses were chilled at 4 °C for the assessment of technological meat quality traits: ultimate pH and $L^*a^*b^*$-color coordinates at 24 h *p-m*.

2.3. Meat quality traits determination

Meat quality indicators were measured according to our previous studies (Gagaoua, Couvreur, Le Bec, et al., 2017; Gagaoua, Picard, & Monteils, 2018; Gagaoua, Terlouw, Micol, et al., 2015). The protocols are briefly summarized here.

For muscle pH at 24 h *p-m*, a Hanna pH meter (HI9025, Hanna Instruments Inc., Woonsocket, RI, USA) was used with a glass electrode suitable for meat penetration. The measurements were done between the 6th and 7th rib. Five measurements were made and the average value was used. The pH meter was calibrated at low temperature (average temperature 3.5 °C) using pH 4 and pH 7 buffers.

For determination of the initial meat color (not color stability), a colorimeter (Minolta CR400, Konica Minolta, Japan) was used to measure meat color coordinates (L^*, a^* and b^*) of the muscles 24 h after slaughter. Fresh cut slices of muscles of at least 2.5 cm thick were left on a polystyrene tray at 4 °C for 1 h to allow blooming prior to color measurement. Color coordinates were calculated using the CIE-LAB system under light source D65 (Daylight), 8 mm diameter measurement area and 10° standard observer. The same colorimeter was calibrated daily according to the standard manual of the manufacturer specifications. For that, the calibration was performed by using standard white tiles (Y = 93.58, x = 0.3150, and y = 0.3217) prior to color determination. L^* (lightness) is measured from 0 (black) to 100 (white), a^* (redness) has a negative value for green and a positive value for red and b^* (yellowness) values have a negative value for blue and a positive value for yellow. Six measurements were taken per slice, an averages were used in the statistical analysis.

Next, Chroma (C^*), related to the intensity of color (higher when a^* of b^* are high), and hue angle (h^*), related to the change of color from red to yellow were calculated using the following equations:

$$C^* = [(a^{*2} + b^{*2})^{1/2}] \quad (1)$$

$$h^* = [(b^*/a^*) \tan^{-1}] \quad (2)$$

2.4. Protein extraction and quantification

Proteins were extracted from frozen muscle samples using a "Precellys 24" tissue homogenizer (Bertin technologies, Saint Quentin-en-Yvelines, France). Briefly, around 80 mg of frozen muscle for each animal was ground using 1.4 mm ceramic beads in a buffer containing 50 mM Tris (pH 6.8), 2% SDS, 5% glycerol, 2 mM DTT, 2.5 mM EDTA, 2.5 mM EGTA, 1× HALT Phosphatase inhibitor (Perbio 78,420), Protease inhibitor cocktail complete MINI EDTA-free (Roche 1,836,170, 1 tablet/10 mL), 2 mM Na_3VO4 and 10 mM NaF. The extracts were then boiled for 10 min at 100 °C, sonicated to reduce viscosity and centrifuged 10 min at 25000*g*. The supernatants were collected and stored at −80 °C until further use. Protein concentrations were determined with a commercial protein assay (Pierce BCA reducing agent compatible kit, ref. 23,252) with BSA as standard.

2.5. RPPA quantification of biomarkers

2.5.1. Antibodies validation

The relative abundances of a list of 29 protein biomarkers candidates previously used to predict beef tenderness, pH and/or color traits (Gagaoua, Bonnet, Ellies-Oury, et al., 2018; Gagaoua, Terlouw, & Picard, 2017; Joseph et al., 2012; Picard et al., 2017; Picard et al., 2018; Wu et al., 2015; Wu et al., 2016) were quantified using specific antibodies. All antibodies had been previously validated for their specificity by western-blot (Fig. 1). The 29 proteins belong to seven biological functions (Table 1):

→ *energy metabolism* (8): Malate dehydrogenase (MDH1), α-enolase 1 (ENO1), β-enolase 3 (ENO3), Retinal dehydrogenase 1 (ALDH1A1), Triosephosphate isomerase (TPI1), Phosphoglycerate kinase 1 (PGK1), Fructose-bisphosphate aldolase (ALDOA) and Glycogen phosphorylase (PYGB)
→ *heat shock proteins* (6): αB-crystallin (CRYAB), Hsp20 (HSPB6), Hsp27 (HSPB1), Hsp40 (DNAJA1), Hsp70-1A (HSPA1A) and Hsp70–8 (HSPA8)
→ *oxidative resistance* (3): Peroxiredoxin 6 (PRDX6), Protein deglycase DJ-1 (PARK7) and Superoxide dismutase [Cu–Zn] (SOD1)
→ *muscle fiber structure* (9): α-actin (ACTA1), α-actinin 2 (ACTN2), α-actinin 3 (ACTN3), MLC-1F (MYL1), Myosin heavy chain-I (MYH7), Myosin heavy chain-IIx (MYH1), Troponin T, slow skeletal muscle (TNNT1), Titin (TTN) and Tubulin alpha-4A chain (TUBA4A)
→ *Cell death, protein binding and proteolysis* (3): Tripartite motif protein

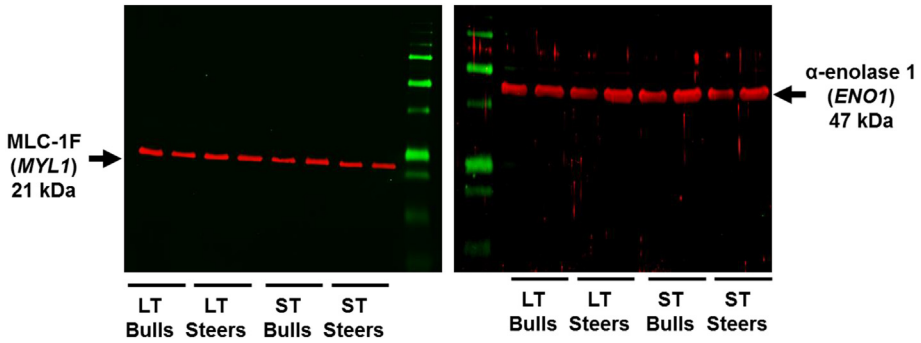

Fig. 1. Example of the strategy used for primary antibodies validation in this study using western blotting.
MLC-F protein (left) was detected using rabbit anti-human MYL1 Abnova (A01) polyclonal primary antibody and ENO1 protein (right) was detected using rabbit anti-human ENO1 Acris BP07 polyclonal primary antibody. Western blot analyses were performed on whole beef muscle extracts from two muscles (*Longissimus thoracis* and *Semitendinosus*) coming from two animal types (bulls and steers). They clearly identified one protein band at the expected molecular weight and this strategy was used for all the antibodies tested in this study (Table 1).
(For interpretation of the references to color in this figure legend, the reader is referred to the web version of this article).

72 (TRIM72), Four and a half LIM domains 1 (FHL1) and μ-calpain (CAPN1)

An antibody was considered specific against the studied protein when only one band at the expected molecular weight was detected by western blot (Fig. 1). Optimal dilution ratios for each of the 29 antibodies were determined at the same time, using routine procedures of validation following the conditions indicated by the supplier of the reactant and adapted to bovine muscle samples (Gagaoua, Terlouw, Boudjellal, & Picard, 2015). Details concerning the proteins and the antibodies used in this study are summarized in Table 1.

2.5.2. Reverse Phase Protein Arrays (RPPA) procedure

After validation of each protein antibody, the RPPA technique was used for the quantification of the biomarkers according to (Gagaoua, Bonnet, Ellies-Oury, et al., 2018). RPPA is a miniaturized immunoassay allowing multiplexed protein analysis (Akbani et al., 2014). Extracted proteins are immobilized on a solid phase with high protein binding capacity per unit area, and are revealed with a specific antibody. Hundreds of samples can be measured at the same time with very high sensitivity and precision from a starting sample volume of only 20 μL. Briefly, the meat extracts of all animals were printed onto nitrocellulose covered slides (Supernova, Grace Biolabs) using a dedicated arrayer (Aushon Biosystems 2470). Four serial dilutions, ranging from 2000 to 250 μg/mL, and two technical replicates per dilution were printed for each sample. Arrays were labeled with 29 specific antibodies (see Table 1 for a complete list of the antibodies references) or without primary antibody (negative control), using an Autostainer Plus (Dako). The slides were incubated with avidin, biotin and peroxydase blocking reagents (Dako) before saturation with TBS containing 0.1% Tween-20 and 5% BSA (TBST-BSA). Slides were then probed overnight at 4 °C with primary antibodies diluted in TBST-BSA. After washes with TBST,

Table 1
List of the 29 protein biomarkers quantified using the Reverse Phase Protein Array (RPPA) technique. The suppliers and conditions for each primary antibody used in this study after western blotting validation are given (Gagaoua, Bonnet, Ellies-Oury, et al., 2018).

Protein biomarkers name (*gene*)	Uniprot ID	Monoclonal (Mo) or Polyclonal (Po) antibodies references	Antibody dilutions
Metabolic enzymes			
Malate dehydrogenase (*MDH1*)	P40925	Mo. anti-pig Rockland 100–601-145	1/1000
α-enolase 1 (*ENO1*)	Q9XSJ4	Po. anti-humanAcris BP07	1/20000
β-enolase 3 (*ENO3*)	P13929	Mo. anti-human Abnova Eno3 (M01), clone 5D1	1/30000
Retinal dehydrogenase 1 (*ALDH1A1*)	P48644	Po. anti-bovine Abcam ab23375	1/500
Triosephosphate isomerase (*TPI1*)	Q5E956	Po. anti-human Novus NBP1–31470	1/50000
Phosphoglycerate kinase 1 (*PGK1*)	Q3T0P6	Po. anti-human Abcam ab90787	1/5000
Fructose-bisphosphate aldolase (*ALDOA*)	A6QLL8	Po. anti-human Sigma AV48130	1/4000
Glycogen phosphorylase (*PYGB*)	Q3B7M9	Po. anti-human Santa Cruz SC-46347	1/250
Heat shock proteins			
αB-crystallin (*CRYAB*)	P02511	Mo. anti-bovine Assay Designs SPA-222	1/1000
Hsp20 (*HSPB6*)	O14558	Mo. anti-human Santa Cruz HSP20–11:SC51955	1/500
Hsp27 (*HSPB1*)	P04792	Mo. anti-human Santa Cruz HSP27 (F-4):SC13132	1/3000
Hsp40 (*DNAJA1*)	P31689	Mo. anti-human Santa Cruz HSP40–4 (SPM251):SC-56400	1/250
Hsp70-1A (*HSPA1A*)	Q27975	Mo. anti-human RD Systems MAB1663	1/1000
Hsp70-8 (*HSPA8*)	P11142	Mo. anti-bovine Santa Cruz HSC70 (BRM22):SC-59572	1/250
Oxidative proteins			
Peroxiredoxin6 (*PRDX6*)	P30041	Mo. anti-human Abnova PRDX6 (M01), clone 3A10-2A11	1/500
Protein deglycase DJ-1(*PARK7*)	Q99497	Po. anti-human Santa Cruz DJ-1 (FL-189):SC-32874	1/4000
Superoxide dismutase [Cu–Zn](*SOD1*)	P00441	Po. anti-rat Acris SOD1 APO3021PU-N	1/1000
Structural proteins			
α-actin (*ACTA1*)	P68133	Mo. anti-Rabbit Santa Cruz α-actin (5C5):SC-58670	1/1000
α-actinin 2 (*ACTN2*)	P35609	Po. anti-human Sigma SAB2100039	1/10000
α-actinin 3 (*ACTN3*)	Q0III9	Po. anti-human Sigma SAB2100040	1/10000
MLC-1F (*MYL1*)	P05976	Po. anti-human Abnova MYL1 (A01)	1/1000
Myosin heavy chain-I (*MYH7*)	P12883	Mo anti-bovine Biocytex 5B9	1/1000
Myosin heavy chain-IIx (*MYH1*)	P12882	Mo anti-bovine Biocytex 8F4	1/500
Troponin T, slow skeletal muscle (*TNNT1*)	Q8MKH6	Po. anti-human Sigma SAB2102501	1/4000
Titin (*TTN*)	Q8WZ42	Mo. anti-human Novocastra NCL-TITIN	1/100
Tubulin alpha-4A chain (*TUBA4A*)	P81948	Mo anti-human Sigma T6074	1/1000
Cell death, protein binding and proteolysis			
Tripartite motif protein 72 (*Trim72*)	E1BE77	Po. anti-human Sigma SAB2102571	1/2000
Four and a half LIM domains 1 (*FHL1*)	Q3T173	Po. anti-human Sigma AV34378	1/5000
μ-calpain (*CAPN1*)	P07384	Mo. anti-bovine Alexis μ-calpain 9A4H8D3	1/500

arrays were probed with horseradish peroxidase-coupled secondary antibodies (Jackson Immuno Research Laboratories, Newmarket, UK) diluted in TBST-BSA for 1 h at room temperature. To amplify the signal, slides were incubated with Bio-Rad Amplification Reagent for 15 min at room temperature. The arrays were washed with TBST, probed with Alexa647-Streptavidin (Molecular Probes) diluted in TBST-BSA for 1 h and washed again in TBST. For staining of total protein, arrays were incubated 15 min in 7% acetic acid and 10% methanol, rinsed twice in water, incubated 10 min in Sypro Ruby (Invitrogen) and rinsed again. The processed slides were dried by centrifugation and scanned using a GenePix 4000B microarray scanner (Molecular Devices). Spot intensity was determined with MicroVigene software (VigeneTechInc).

2.5.3. Protein intensity calculation and normalization

The relative abundances of proteins were determined according to the following procedure. First, raw data were normalized using NormaCurve (Troncale et al., 2012), a SuperCurve-based method that simultaneously quantifies and normalizes Reverse Phase Protein Array data for fluorescent background per spot, a total protein stain and potential spatial bias on the slide. Next, each RPPA slide was median centered and scaled (divided by median absolute deviation). We then corrected for remaining sample loading effects individually for each array by correcting the dependency of the data for individual arrays on the median value of each sample over all the arrays using a linear regression.

2.6. Statistical analyses

Statistical analyses were conducted using SAS statistical software (SAS 9.1, SAS Institute INC, Cary, NC, USA) and XLSTAT 2017.19.3 (AddinSoft, Paris, France). Before analysis, raw data means were scrutinized for data entry errors and outliers. Shapiro-Wilk tests were used to determine the normality of data distribution. Values were expressed as the mean ± standard deviation (SD). The PROC CORR of SAS was used to compute the Pearson's correlation coefficients between the 29 biomarkers, ultimate pH and color traits. Correlation values were considered significant at $P < 0.05$. Multiple regression analyses were performed using the PROC REG of SAS to create best models for pH and color coordinates (as dependent variables, x) using the protein biomarkers (as independent variables, y). For modeling, we used our recently described statistical approach (Gagaoua, Couvreur, Le Bec, et al., 2017; Gagaoua, Terlouw, Micol, et al., 2015). Briefly, the option "optimal model" was chosen to produce the model with the highest r^2 value. We maximized the number of the explanatory variables to be retained in the models at 4 to meet the principle of parsimony [one variable each ten observations (animals)]. Variables that were significant but contributed < 2% in terms of explanatory power (r^2) were excluded. Partial R-squares, regression coefficients, t-values, and significance of each retained variable were calculated. The absence of collinearity was systematically verified for each regression model, by producing condition indices and variance proportions using the COLLIN procedure of SAS. Variables were identified as collinear if they possessed both a high condition index (> 10) and a proportion of variation of > 0.5 for two or more traits (Gagaoua et al., 2016). If collinearity was detected, the variable was removed from the model in a stepwise manner.

For better identification of the mechanisms and thus pathways that drive beef color traits, a principal component analysis (PCA) combined with k-means (Gagaoua, Couvreur, Le Bec, et al., 2017; Gagaoua, Monteils, Couvreur, & Picard, 2017) was performed to create color classes following the validation procedure described recently (Gagaoua, Picard, Soulat, & Monteils, 2018). PCA allows the visualization of the distribution of the color coordinates (L^*, a^*, b^*, C^* and h^*) and the factor loading scores of individual animals were used for creating classes. For this, a k-means cluster analysis ($k = 3$) was undertaken. K-means clustering is a widely used classification method that generates a specific number of classes (nonhierarchical). This method assumes a certain number of clusters, k, fixed *a priori* and produces a separation of the objects into non-overlapping groups coming from Euclidean distances minimized at each step of an iterative procedure. We proceeded by using the variability explained by the axes of the PCA with eigenvalues > 1.0 after Z-scores calculation (Gagaoua, Monteils, Couvreur, & Picard, 2017). Two factors with eigenvalues > 1.0 were extracted on the basis of the scree plot and evaluation of the factor loading matrix after orthogonal rotation. An eigenvalue represents the amount of variance that is captured by a given component. Eigenvalue criterion is one of the most commonly used criteria for solving the number of components problem, also known as the Kaiser-Guttman criterion (Kaiser, 1974). To check the suitability of the factorial model, the Kaiser-Meyer-Olkin (KMO) test for sampling adequacy was used. The Euclidean matrix distance was applied to classify meat samples into 3 classes according to their color characteristics, hence to simplify the comparisons we named them "pale red", "light red" and "dark red" classes and used this terminology throughout the manuscript.

The classes were compared using the PROC GLM procedure of SAS for both their technological traits and protein biomarker relative abundances given in Table S1. Significant differences between classes were performed using Tukey's test at a significance level of $P < 0.05$. In addition, PCAs were carried out using the correlated biomarkers with each color coordinate by the projection of the animals belonging to each meat color class as supplementary variables. They aimed to illustrate visually the correlated biomarkers (Plots containing only factor loadings of variables) with each color quality trait in relation to the classes barycenters (bi-plots containing factor loadings of variables as well as factor loading scores of the 3 beef color classes). Further, an additional PCA was performed using the dependent variables and the differential proteins to obtain a more complete picture of the differences according to the barycenters of the classes.

3. Results and discussion

3.1. Meat color and pH parameters

The mean values (± SD) of meat color coordinates are given in Table S2. The findings indicate that L^*-values (31.5 ± 4.98) are slightly lower than those reported for LT muscle of young animals, where the average was reported to be 35–37 for bulls of 12–18 months old, including the Charolais breed (Priolo, Micol, & Agabriel, 2001). a^*-values (16.2 ± 3.74) and b^*-values (17.0 ± 3.85) were slightly higher than those described by our earlier studies for young bulls of similar age slaughtered under the same conditions (Chambaz, Scheeder, Kreuzer, & Dufey, 2003; Gagaoua, Terlouw, Micol, et al., 2015). These differences may be related to myoglobin contents that were further different for these animals (data not shown). Earlier studies reported that haem iron content of muscle increases with age especially up to 24 months of age and then remains relatively stable (Renerre, 1990). It is possible that several factors other than age were responsible for the variation and differences in color from pale to dark meat for Charolais bulls as these animals were reared with low physical activity. Indeed, some authors consider the animal physical activity as a possible factor affecting meat color (Dunne, Keane, O'Mara, Monahan, & Moloney, 2004). The observed findings of meat color may be also related to muscle metabolic activity such as isocitrate dehydrogenase (ICDH) as previously reported (Gagaoua, Monteils, Couvreur, & Picard, 2017; Gardner et al., 2007). The LT muscle of young Charolais bulls (15–24 months) is known to contain high proportions of MyHC-I fibers with high ICDH and low lactate dehydrogenase activities (Jurie et al., 2005). Ultimate pH would influence the final color (Dunne et al., 2004; Gagaoua, Picard, & Monteils, 2018). In the present work, the mean pH value was 5.62 ± 0.09. During loading, transport and handling at the experimental slaughterhouse, great care was taken of the animals in order to avoid stress and thus keep the pH values within the normal range for

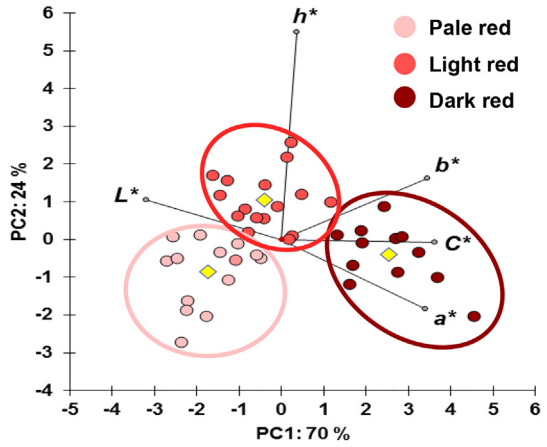

Fig. 2. Projection of the three meat color classes (pale, light and dark red) of *Longissimus thoracis* muscle of young Charolais bulls categorized by the iterative procedure *K*-means after principal component analysis (PCA) on the five color coordinates: L^*: lightness, a^*: redness, b^*: yellowness, C^*: Chroma and h^*: hue angle. The barycenter (centroid) of each class (pale (n = 15), light (n = 16) and dark (n = 12) red meat classes) is shown with yellow lozenges. Individuals belonging to the same class are encircled in clusters using the corresponding schematic colors. The overall Kaiser-Mayer-Olkin score of the PCA was 0.82 (Bartlett's test of sphericity was significant, $P < 0.001$). (A colored version of the figure is available online).

beef. When the pH after 24 h *p-m* is higher than 6.0, the meat could be downgraded due to its inacceptable color. In this study, for all the young Charolais bulls, the final pH was below the threshold of 6.0 and ranged from 5.51 to 5.92 (only 3 animals had pH between 5.8 and 5.92), which is an adequate value for beef as it follows normal *post-mortem* metabolism (Gagaoua, Picard, & Monteils, 2018; Gagaoua, Picard, Soulat, & Monteils, 2018; Matarneh, England, Scheffler, & Gerrard, 2017).

3.2. Relationships among meat color traits and animal classes

The significant correlation and regression relationships between meat color traits are presented in Figs. 2 and 3. Only variables with statistically significant correlations are shown in Fig. 3. L^*-values were negatively correlated ($-0.72 < r < -0.79$; $P < 0.001$) with a^*, b^* and C^*-values. As expected, a^*-values were positively correlated with b^*-values ($r = 0.79$; $P < 0.0001$). The results indicate that none of the color coordinates were related with ultimate pH ($-0.02 < r < 0.20$; $P > 0.20$). The absence of correlation is consistent to our recent findings for French young Blond d'Aquitaine bulls (Gagaoua, Terlouw, Micol, et al., 2015) and can be explained by final pH values that were within the normal and narrow range. Hence, it may be suggested that final pH is neither the only nor the most important factor influencing the analyzed beef color traits as recently postulated (Calnan, Jacob, Pethick, & Gardner, 2016).

The PCA-*k*-means summarized the projection of meat color traits and animal loadings (Fig. 2). This approach allowed the clustering of the animals according to their color traits. Thus, we identified three clusters based on the average silhouette width (*Si*) criterion (Gagaoua, Picard, Soulat, & Monteils, 2018) and named them “pale red”, “light red” and “dark red” meat groups, respectively. This terminology was used throughout this manuscript and highlighted in the graphs using the corresponding colors when necessary. The purpose of this categorization was i) to facilitate the discussion of the results; ii) to show the tendencies for relationships of the biomarkers with the color traits according to the characteristics of the clusters (Fig. 2) and to highlight the individual variability within animals from the same batch. The two first PCs accounted for 94% of the total variance, with the first and second components explaining 70% and 24% of the total variability,

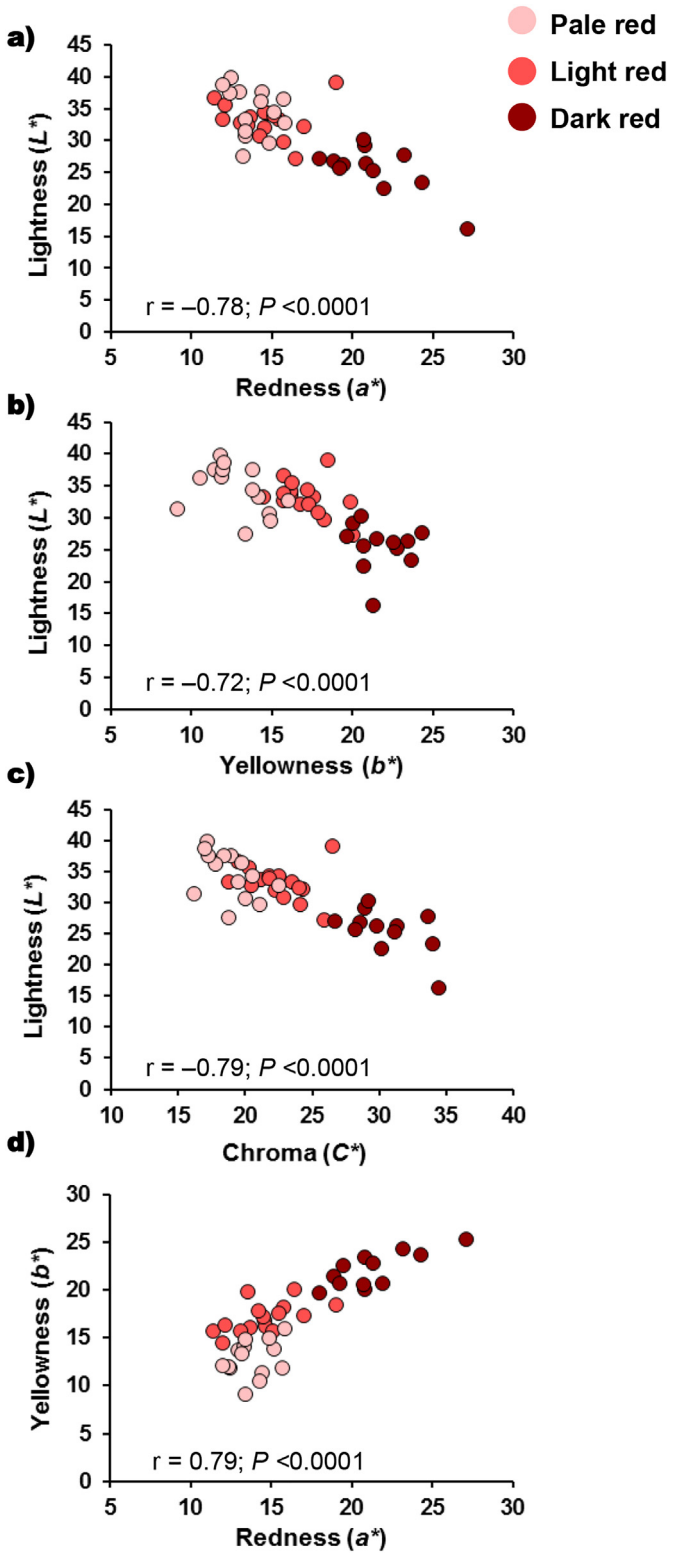

Fig. 3. Pearsons correlations between color parameters.
a) between L^* and a^*; b) between L^* and b^*; c) between L^* and C^* and d) between b^* and a^*. (A colored version of the figure is available online).

respectively. In agreement to the results presented above, the first PC was positively correlated with a^*, b^* and C^* and negatively with L^*. The second PC was positively correlated with h^* only. This is in agreement with the projection of the color coordinates of Charolais breed irrespective of the sex (Gagaoua, Picard, & Monteils, 2018). On

Table 2
Least square of the means (± SD) of the instrumental meat color and ultimate pH for *Longissimus thoracis* muscle of meat color classes created for the 43 pure young Charolais bulls.

Parameters	Pale red[1] (n = 15)	Light red (n = 16)	Dark red (n = 12)	SEM[2]	*P*-value[3]
Lightness (*L**)	34.5^{a} (3.61)	33.0^{b} (2.65)	25.6^{c} (3.49)	0.76	***
Redness (*a**)	13.8^{c} (1.20)	14.7^{b} (1.91)	21.3^{a} (2.45)	0.57	***
Yellowness (*b**)	12.8^{c} (1.82)	17.4^{b} (1.49)	21.8^{a} (1.47)	0.61	***
Chroma (*C**)	18.9^{c} (1.71)	22.8^{b} (2.12)	30.5^{a} (2.36)	0.78	***
Hue angle (*h**)	42.7^{c} (4.20)	49.8^{a} (2.96)	45.7^{b} (2.95)	0.74	***
Ultimate pH	5.57^{c} (0.03)	5.69^{a} (0.12)	5.62^{b} (0.06)	0.01	**

[1] Least square means in the same row for meat color classes not followed by a common letter (a–c) differ significantly at $P < 0.05$.
[2] Standard error of mean.
[3] Significance levels: $^{**}P < 0.01$; $^{***}P < 0.001$.

the positive side of the first PC are loaded the animals characterized by dark meat with the highest *C**-values (Table 2). The *C** index represents the color intensity and is a good blooming indicator in fresh meat exposed to air. Inversely, on the negative side are loaded the animals characterized by pale red meat with the highest *L**-values as can be seen in Table 2. The animals characterizing light red meat are mainly loaded on the center and top of the first and second PCs, respectively. The variable of pH values was removed from the PCA, because it loaded less (factor loading < 0.50) with a very bad Kaiser-Mayer-Olkin score (KMO = 0.42). The eligible variables should obtain KMO values that exceed 0.5.

3.3. Relationships between biomarker abundances in the early post-mortem period and ultimate pH

The correlation analyses showed that ultimate pH was correlated with 6 proteins from muscle extracts sampled at 45 min *p-m* (Table 3). The proteins belong to three biological pathways and half of them are metabolic enzymes: ENO1, ENO3 and TPI1. The activity of metabolic enzymes is of biological significance for meat quality development and pH. In the *p-m* muscle, the anoxia situation caused by the sudden cut of blood flow drastically reduces energy production. The course of glycolysis determines the final pH value, which, in consequence, affects the quality traits of meat. Earlier studies indicated the involvement of several proteins belonging to energy metabolism in *p-m* conversion of muscle into meat (Jia et al., 2006; Picard et al., 2014; Picard et al., 2017), which thus explain the relation with final pH. Recent reports suggest that this shift may also be related to protein phosphorylation (for review see (Chauhan & England, 2018; England, Matarneh, Scheffler, & Gerrard, 2017; Ouali et al., 2013), which would indirectly affect the extent and rate of pH decline. For example, the phosphorylation of TPI1 was reported to correlate with the rate of *p-m* pH decline (Huang et al., 2011). TPI1 catalyzes the interconversion of dihydroxyacetone phosphate and glyceraldehyde 3-phosphate. The latter is the substrate directly involved in the glycolytic pathway. The positive associations with enolases may reflect a cellular stress response to the deprivation of oxygen supply and to glucose metabolism (low glucose levels) (Sedoris, Thomas, & Miller, 2010). ENO1 and ENO3 are two isoforms catalyzing the conversion of 2-phosphoglycerate to phosphoenolpyruvate and leading to an increased rate of glycolysis and meat quality variation (Gagaoua, Terlouw, Micol, et al., 2015; Jia et al., 2006). Finally, these three metabolic and glycolytic enzymes are found predominantly in muscle tissue and their increased activity just after slaughter might correlate with the decrease of pH due to lactate accumulation. Thus, a prolonged ATP generation *via* glycolysis contributes to both lactate and hydrogen ion accumulation. Extensive reviews on this topic are available (England et al., 2017; Matarneh et al., 2017; Ouali et al., 2013).

Three other proteins were found to correlate with pH, of which two were structural proteins: the giant protein Titin (TTN) and α-actin. TTN was earlier reported to be related to pHu (Farouk, Mustafa, Wu, & Krsinic, 2012). The correlation of α-actin and μ-calpain with pHu was also previously reported for beef (Gagaoua, Couvreur, Le Bec, et al., 2017) and pork (Kwasiborski et al., 2008). Furthermore, in coherence with our data, proteomic studies found that the onset of apoptosis is followed by actin degradation, which is related to pH drop (Gagaoua, Terlouw, Micol, et al., 2015). Accordingly, pHu was linked to μ-calpain, which is also related to α-actin ($r = 0.58$; $P < 0.001$). Overall, these observations are in agreement with hypotheses proposing alterations in

Table 3
Pearson correlations between pHu, color parameters and protein biomarkers quantified by RPPA technique on *Longissimus thoracis* muscle of the 43 young Charolais bulls. Only the significant correlations are shown.

Protein biomarkers[a]	Ultimate pH	Lightness (*L**)	Redness (*a**)	Yellowness (*b**)	Chroma (*C**)	Hue angle (*h**)	Total correlations
Metabolic enzymes							
MDH1		+0.28^{t}		−0.30*			2
ENO1	+0.39*	−0.29^{t}					2
ENO3	+0.36*						1
ALDH1A1			+0.33*			−0.34*	2
TPI1	+0.31*			+0.28^{t}			2
Oxidative and stress proteins							
Hsp20			+0.31*		+0.30*		2
SOD1			+0.41**	+0.30*	+0.38**		3
Structural proteins							
α-actin	−0.28^{t}	+0.42**	−0.37*	−0.54***	−0.49***	−0.32*	6
α-actinin 3				−0.32*			1
MHC-I						−0.35*	1
MHC-IIX			−0.42**	−0.30*	−0.37*		3
TTN	+0.28^{t}	−0.34*	+0.41**	+0.54***	+0.50***		5
Cell death, protein binding and proteolysis							
TRIM72		−0.31*					1
FHL1		−0.29^{t}	+0.33*		+0.27^{t}		3
μ-calpain	−0.29^{t}			−0.29^{t}		−0.33*	3
Total correlations	6	6	7	8	6	4	

Significance levels: t $P < 0.06$.
* $P < 0.05$.
** $P < 0.01$.
*** $P < 0.001$.
[a] The proteins biomarkers are listed depending on metabolic pathways they belong.

Table 4
Regression equations (optimal models) of meat color coordinates and pHu of *Longissimus thoracis* samples from young Charolais bulls using protein biomarkers quantified by RPPA.

Dependent variable	R-squared[a]	S.E	Entered independent variable[b]	Partial R[b]	Regression coefficient	*t*-value	*P*-value
Lightness (*L**)	0.44***	0.18	TTN	0.17	−0.41	−2.30	0.015
		0.13	Trim72	0.15	−0.39	−2.93	0.006
		0.15	MHC-I	0.08	+0.34	+2.35	0.053
		0.18	PRKG1	0.04	−0.27	−1.55	0.018
Redness (*a**)	0.50***	0.12	SOD1	0.17	+0.47	+3.75	0.004
		0.13	TTN	0.24	+0.38	+2.87	0.000
		0.13	FHL1	0.05	+0.25	+1.95	0.057
		0.12	Hsp20	0.04	+0.21	+1.69	0.015
Yellowness (*b**)	0.59***	0.12	TTN	0.29	+0.74	+6.19	0.000
		0.11	SOD1	0.16	+0.48	+4.20	0.000
		0.11	Hsp40	0.08	+0.30	+2.65	0.033
		0.12	α-Tubulin	0.06	−0.26	−2.22	0.012
Chroma (*C**)	0.55***	0.12	TTN	0.25	+0.59	+4.93	0.000
		0.13	SOD1	0.22	+0.47	+3.57	0.001
		0.12	Hsp40	0.05	+0.24	+2.04	0.049
		0.12	MHC-IIx	0.03	−0.19	−1.51	0.022
Hue angle (*h**)	0.44***	0.15	MHC-I	0.12	−0.44	−2.95	0.000
		0.15	TTN	0.15	+0.58	+3.83	0.005
		0.14	ALDH1A1	0.09	−0.31	−2.20	0.034
		0.14	FHL1	0.08	−0.29	−2.15	0.039
Ultimate pH	0.37**	0.15	ENO3	0.13	+0.47	+3.22	0.002
		0.15	αB-crystallin	0.08	+0.41	+2.75	0.009
		0.14	μ-calpain	0.09	−0.30	−2.11	0.035
		0.14	Hsp40	0.07	−0.27	−1.92	0.042

[a] Significance levels of the models: **P < 0.01; ***P < 0.001.
[b] Variables are shown in order of their entrance in the regression models.

the extent and rate of pH decline may induce conformational changes leading to the activation and/or liberation of molecules (*e.g.,* Ca^{2+}) able to play pivotal roles in myofibrillar proteins degradation (Huff-Lonergan, Zhang, & Lonergan, 2010).

For a better understanding of the biological mechanisms related to ultimate pH, multivariate regression analyses were conducted (Table 4). Four proteins [ENO3 and αB-crystallin (positive) and μ-calpain and Hsp40 (negative)] explained 37% of the variability of ultimate pH (Table 4). The low predictive power of pH models in our study was consistent with that reported by (Liu, Lyon, Windham, Lyon, & Savage, 2004) and (Gagaoua, Couvreur, Le Bec, et al., 2017). These authors argued that the low predictive ability of equations for pH might be related to the low variation of measures of this trait. Furthermore, it is important to emphasize that protein biomarkers do not predict and measure pH directly as is the case with H^+ sensitive electrodes, but they may explain the biological mechanisms behind the *p-m* pH decline. Accordingly, the best equation obtained in this study reveals the involvement of two Hsp proteins (αB-crystallin and Hsp40), thus confirming the previously reported link in bulls between pHu and cellular stress (Pulford et al., 2009). A recent study by the same group reported that small Hsp proteins bind to damaged or degraded myofibrillar proteins, which prevents calpains to efficiently exert their proteolytic activity (Lomiwes, Farouk, Frost, Dobbie, & Young, 2013) or to be used as specific substrates by these calcium-dependent proteases (Gagaoua, Terlouw, Micol, et al., 2015). These associations are likely to be pH compartmentalized, hence affecting the final aspects of meat quality including color as previously reported for beef tenderness (Lomiwes, Farouk, Wu, & Young, 2014). In addition, since the *p-m* muscle acidification is accompanied by the inversion of acidic phospholipids from external and neutral phospholipids to internal, we suggested that Hsps would play different roles in the membrane function and pH decline (Gagaoua, Terlouw, Micol, et al., 2015). These may involve apoptosis and perhaps other mechanisms not yet identified. Thus, elucidating the molecular link between muscle proteome and meat quality traits by relating multiple proteins, *i.e.,* interactomics, is obviously more accurate than looking at a single protein.

3.4. Relationships between biomarker abundances in the early post-mortem period and meat color coordinates

The correlations observed between the relative abundances of biomarkers and meat color traits are summarized in Table 3. A Venn diagram in Fig. S1 grouped all the correlations. Fourteen proteins were significantly correlated with color coordinates and 5 were common with pHu.

Interestingly, the results showed that α-actin was correlated with all color coordinates (positively with *L** and negatively with *a**, *b**, *C** and *h**) including pHu (Table 3). This protein discriminated efficiently the 3 color classes (Fig. S2a,b). α-actin is among the structural proteins already identified by proteomic investigations to be related with meat color (Gagaoua, Couvreur, Le Bec, et al., 2017; Gagaoua, Terlouw, Micol, et al., 2015; Hwang et al., 2005; Polati et al., 2012). In this study, this structural protein was 6.20-fold more abundant in pale red compared to dark red meat class. This marker of *p-m* muscle apoptosis (Ouali et al., 2013) was further reported by our group to be more abundant in the tender class of young Charolais, Limousin and Blond d'Aquitaine bulls (Chaze et al., 2013). Thus, once proteolysis progressed and proteins were degraded by μ-calpain and other proteases (such as caspases), a profound ultrastructural change takes place in the original structure of meat, which may influence meat color aspects. The involvement of this protein in meat color could be related to the light scattering of meat. A comprehensive review by (Hughes, Oiseth, Purslow, & Warner, 2014) detailed this phenomena and proposed that the extent of light scattering could be influenced by the structural attributes of the muscle that would contribute to the perceived lightness as viewed by the eye.

TTN was correlated with 4 color traits (negatively with *L** and positively with *a**, *b** and *C**) and allowed to further distinguish the color classes (Fig. S2c,d). This protein entered in all the regression equations (negative for *L** and positive for *a**, *b**, *C** and *h**) and alone explained from 15 to 29% of variability (Table 4). TTN, also called connectin, belongs to the most important proteins responsible for meat tenderization (Fritz & Greaser, 1991). In the A-zone of the sarcomere, TTN is bound to myosin filaments. In the I-zone of the sarcomere, some regions

of the TTN molecule interact with thin (actin) filaments (Gregorio, Granzier, Sorimachi, & Labeit, 1999). Furthermore, these authors reported that phosphorylation of TTN was found in different parts of this giant molecule, from the M-line to the *Z*-disc of the sarcomere. Earlier studies found that TTN underwent partial degradation directly after slaughter and that further degradation took place during the first 24 h *p-m* (Taylor, Geesink, Thompson, Koohmaraie, & Goll, 1995). Based on the comprehensive review by (Huff-Lonergan & Lonergan, 2005), degradation of costamere linkages during *p-m* ageing will reduce myofibril shrinkage, leaving more space within muscle fibers to retain water, which would affect the light scattering of muscle structure. According to these authors, degradation of proteins such as TTN may disrupt the integrity of the myofibril. This degradation and involvement of water might affect the texture, light scattering and final aspect of meat quality, including meat color (Hughes et al., 2014; Hughes, Clarke, Purslow, & Warner, 2017). Furthermore, an earlier work based on pH-related muscle proteome alterations revealed structural-contractile proteins participate in these changes, namely in the *Longissimus thoracis* bovine muscle conversion to DFD meat (Franco et al., 2015). Overall, the findings with TTN and *Z*-disc proteins may explain the relationships with color parameters and pH decline as discussed above. Furthermore, because TTN is bound to thick filaments in the A-band and to thin filaments in the Z-disk (Funatsu et al., 1993), rotation of thin filaments by the crossbridges must inevitably lead to winding of TTN upon them, leading to the production of torque in α-actinin that would affect meat color. According to the findings of this report, one could propose α-actin and TTN to be strongly related with the biological pathways driving meat color development of young Charolais bulls. Nevertheless, the mechanism by which TTN may affect meat color is still unclear and further investigations are needed using accurate techniques.

The biomarkers that were significantly correlated with color traits were introduced into PCAs (Fig. 4a-d) by projecting the barycenters of the corresponding meat color classes. The variability explained by the first two PCA axes of L^* (Fig. 4a), a^* (Fig. 4b), b^* (Fig. 4c) and C^* and h^* together (Fig. 4d) were 56.3%, 54.4%, 58.1% and 43.7%, respectively. The visualization of the relationships within color classes was possible thanks to PCA axes. The power of TTN, α-actin, MyHC-IIx, μ-calpain and α-actinin to discriminate the meat color classes is of great significance (Fig. 5a,b). The scatterplots of Fig. 5b highlight the abundance differences in TTN, α-actin and MyHC-IIx between the 3 color classes. Additional proteins were found with high discriminative power, and this included α-actinin. This protein is a major component of the Z-disk and strongly associates with actin filaments and structural proteins to stabilize the cytoskeleton (Raynaud et al., 2003). The location of a μ-calpain binding site in the C-terminal region of α-actinin situates the protease in the vicinity of TTN (Ohtsuka, Yajima, Maruyama, & Kimura, 1997), a protein described as an α-actinin partner in the Z-line and known as a calpain substrate (Papa et al., 1999). In addition to the structural proteins, μ-calpain allowed efficient discrimination between meat color classes (Fig. 5a). Note that these three proteins strongly participate in Z-disk organization, a compartment which rapidly undergoes proteolysis during muscle ischemia or after a calpain treatment of isolated myofibrils (Raynaud et al., 2003). From these findings concerning structural proteins, we suggest their variation in abundance modifies the degree of light penetrating the structural elements and thereby meat color. Accordingly, Warner's group proposed using reflectance confocal laser scanning microscopy the detailed mechanisms by which visual aspects of meat color would be affected in relation to fiber type (Hughes et al., 2017). Thus, we emphasize muscle fiber type proportions may influence the amount of free water and structural modifications caused by the proteolytic processes following apoptosis and consequently, light reflectance and scattering properties of the meat. Overall, these findings support the hypothesis from (Hughes et al., 2014) suggesting that meat color is not only determined by the pigment, but is also influenced by muscle structure. According to the findings of this report, we suggest that this hypothesis would depend on the individual variability among muscles, breeds and animal-types.

Because the reflectance aspects of meat color are influenced by protein denaturation, interaction with heat shock proteins (Hsps) may defer changes in the structure of pigment and myofibrillar proteins (Gagaoua, Terlouw, Micol, et al., 2015). In agreement with the role of apoptosis in muscle to meat conversion (Gagaoua et al., 2015), members of the small Hsp protein family were positively involved. Hsp20 was associated with a^* and C^*-values (Fig. 4b,d). It loaded exclusively within the light and dark red classes characterized by the highest pHu, in contrast to the pale red class (Table 2). This may be explained by the ability of Hsp20 to control the redox status. For example, in exercising muscles, increased levels of small Hsp were associated with lower levels of thiobarbituric acid reactive substances, suggesting that these proteins may lower oxidative stress status (Jammes, Steinberg, Delliaux, & Bregeon, 2009). Hsp40 was also positive in the regression equations of meat color coordinates of b^* and C^*. The primary studies have shown negative relationships between *DNAJA1* (the gene coding for Hsp40 protein) expression in *Longissimus thoracis* muscle and tenderness (Bernard et al., 2007). Subsequently, this protein was reported by our group to be related to beef color (Gagaoua, Couvreur, Le Bec, et al., 2017; Gagaoua, Terlouw, Micol, et al., 2015; Gagaoua, Terlouw, & Picard, 2017). Hsp40 is a co-chaperone that would assist the regulation of complex formation between Hsp70 and client proteins using rapid and transient interaction by activating ATP hydrolysis (Liu & Steinacker, 2001). Changes in Hsp40 expression might reflect the involvement of muscle metabolism (Cassar-Malek et al., 2011). This may partly explain why it is retained in meat color development, in addition to its protective role on muscle structure. However, there are few studies exploring the relationship of Hsps with meat quality (Gagaoua, Terlouw, Monteils, Couvreur, & Picard, 2017) including meat color development and the underlying mechanisms by which they act in stability of meat color is not understood in detail yet.

Among the antioxidant proteins linked with color coordinates, we validated SOD1. It was, as expected, positively correlated with a^*, b^* and C^* (Table 3 and Fig. S1) and retained in their regression equations, explaining from 16 to 22% of variability (Table 4). This protective scavenger protein has been related to the preservation of meat color stability during *post-mortem* storage (Wu et al., 2015) and correlated with meat color of different species (Gagaoua, Terlouw, Micol, et al., 2015; Gao, Wu, Ma, Li, & Dai, 2015). As an antioxidant protein, SOD allows a fast dismutation of O_2^- to O_2 and H_2O_2. It is among the defense mechanisms that were suggested to protect mitochondria against lipid peroxidation and reactive oxygen species, known to be very detrimental to meat color stability. The oxidation of polyunsaturated membrane lipids in *p-m* muscle may also cause a loss of fresh meat color (Gagaoua, Terlouw, Micol, et al., 2015). In Charolais cattle, meat color has a close association with lipid oxidation through the balance between pro- and anti-oxidant substances (Gatellier, Mercier, Juin, & Renerre, 2005). Thus, we hypothesize that SOD may play a major role to counteract the discoloration phenomena and protect cells from oxidative stress together with other proteins, for instance heat shock proteins.

In the present study, 6 metabolic enzymes were related with color coordinates. They were all reported by previous proteomic studies to associate with meat color: ENO1 by (Kwasiborski et al., 2008), MDH1 by (Gagaoua, Terlouw, Micol, et al., 2015; Gao et al., 2015), TPI1 by (Nair et al., 2016; Wu et al., 2015), ALDH1A1 by (Wu et al., 2016), PRKG1 by (Wu et al., 2015) and PYGM by (Wu et al., 2016). Of these, only ENO1 and TPI1 were additionally related to ultimate pH. It is admitted that the rate and extent of *p-m* energy metabolism is a major regulatory molecular mechanism underlying both pH and fresh meat color (England et al., 2017). Our findings support the growing consensus that metabolic enzymes, namely those of glycolysis, play important roles in the meat ageing process by influencing both pH decline and fueling of complex energy-dependent mechanisms, namely those of apoptosis and autophagy (Nikoletopoulou, Markaki, Palikaras, & Tavernarakis, 2013). The enzymes listed above produce a myriad of

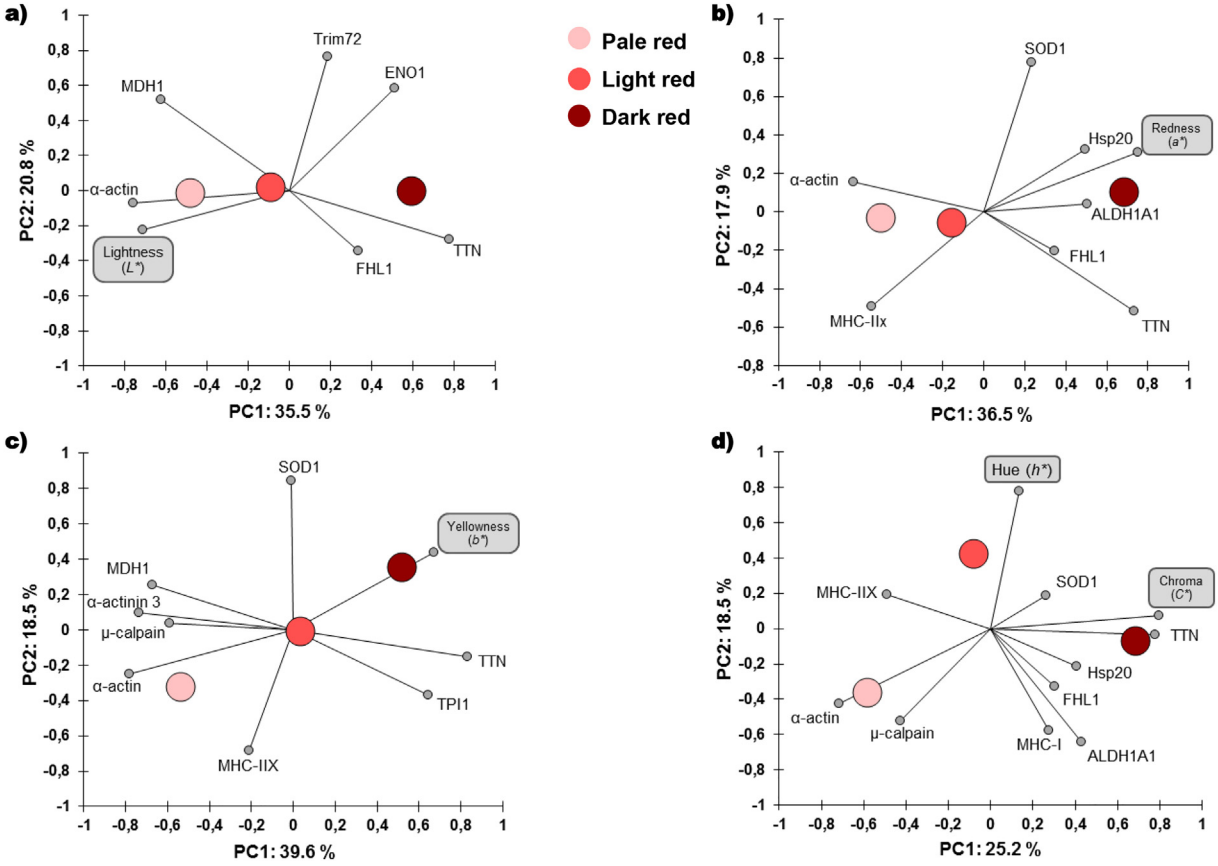

Fig. 4. Representation of the PCAs showing relationships (from Table S3 and Fig. 4) between the color coordinates a) Lightness, b) Redness, c) Yellowness), d) Chroma and hue angle with the significantly correlated biomarkers on *Longissimus thoracis* muscle of young Charolais bulls.
The distribution of pale, light and dark red meat classes by their barycenters (centroids) are shown with circles using the corresponding schematic colors. For all PCAs, the overall KMO was > 0.70 (with no variable with a KMO < 0.50) and thus the obtained data were suitable for a factor analysis. (A colored version of the figure is available online).

metabolites, such as lactate, succinate, malate, and pyruvate. The influence of these metabolites on fresh meat color and myoglobin stability occur primarily through their interactions with mitochondria (phosphorylation, apoptosis and fusion/fission mechanism) and enzyme systems, which lead to NADH replenishment and subsequent metmyoglobin reduction. Some of the validated enzymes may also play added biological roles. Besides their function in glycolysis by the conversion of glyceraldehyde to 2-phosphoglycerate (Jia et al., 2006), some members of the complex aldehyde dehydrogenase family (ALDH1A1) could also protect cells against cytotoxic effects of various aldehydes accumulating in the cytosol (Vasiliou, Thompson, Smith, Fujita, & Chen, 2012). These enzymes can easily detoxify 4-hydroxynonenal (HNE) and malondialdehyde (MDA), two major products of lipid peroxidation generated during oxidative stress. Furthermore, ALDH1A1 is involved in the metabolism of vitamin A (by oxidation of retinol) and participates in the second and third lines of antioxidant defense (Duester, 2000).

Other unusual proteins identified for the first time correlated with meat color including FHL1 and TRIM72, and these were negatively related to L^*-values. FHL1 was further positively related with a^* and C^*-values (Tables 3 and 4). Four and a half LIM domains 1 (FHL1) regulates gene transcription, cell proliferation, metabolism and apoptosis (Shathasivam, Kislinger, & Gramolini, 2010). The LIM domain forms a tandem zinc-finger structure that provides a modular protein-binding interface, through which FHL1 functions as adaptor or scaffold to support the assembly of multimeric protein complexes and regulates the localization and activity of their partners (Shathasivam et al., 2010). This protein is confined to the *Z*-line of skeletal muscle and its proteolysis is linked to the release of intact α-actinin from bovine myofibrils and contributes to the weakening of the Z-line during meat tenderizing (Morzel et al., 2004). FHL1 may also interact with other biological pathways, namely metabolic enzymes (Lange et al., 2002) in response to both hypoxia and oxidative stress (Gagaoua, Hafid, Boudida, et al., 2015), which may explain its loading within the dark red classes characterized by low glycolytic properties (Fig. 5) and high levels of ALDH1A1, MHC1, Hsp20 and SOD1 (Fig. 4d) (Picard et al., 2018). In the same manner, Tripartite motif-containing 72 (TRIM72), which is exclusively expressed in skeletal muscle, might act as a sensor of oxidation on membrane damage (Cai et al., 2009), thereby influencing meat color aspects. The negative relation between TRIM72 and L^* confirms the anti-oxidative properties of this protein (Jung & Ko, 2010), which may contribute to the clearance of harmful agents that accumulate during apoptosis. Further investigations are needed to clarify the roles of these two proteins in relation to meat quality traits and color development/stability.

4. Conclusion

In the present report, we implemented for the first time RPPA for the quantification of a dozen proteins on a large number of beef samples, in order to relate them with meat quality traits (herein ultimate pH and color parameters). The results highlighted the importance of several biological pathways in muscle to meat conversion, and consequently of meat color. Thanks to the use of RPPA, the validation of the importance of several proteins was made possible in this study. Structural proteins, likely α-actin, TTN, α-actinin, MyHC-IIx and others, were validated as efficient candidate biomarkers of meat color. These

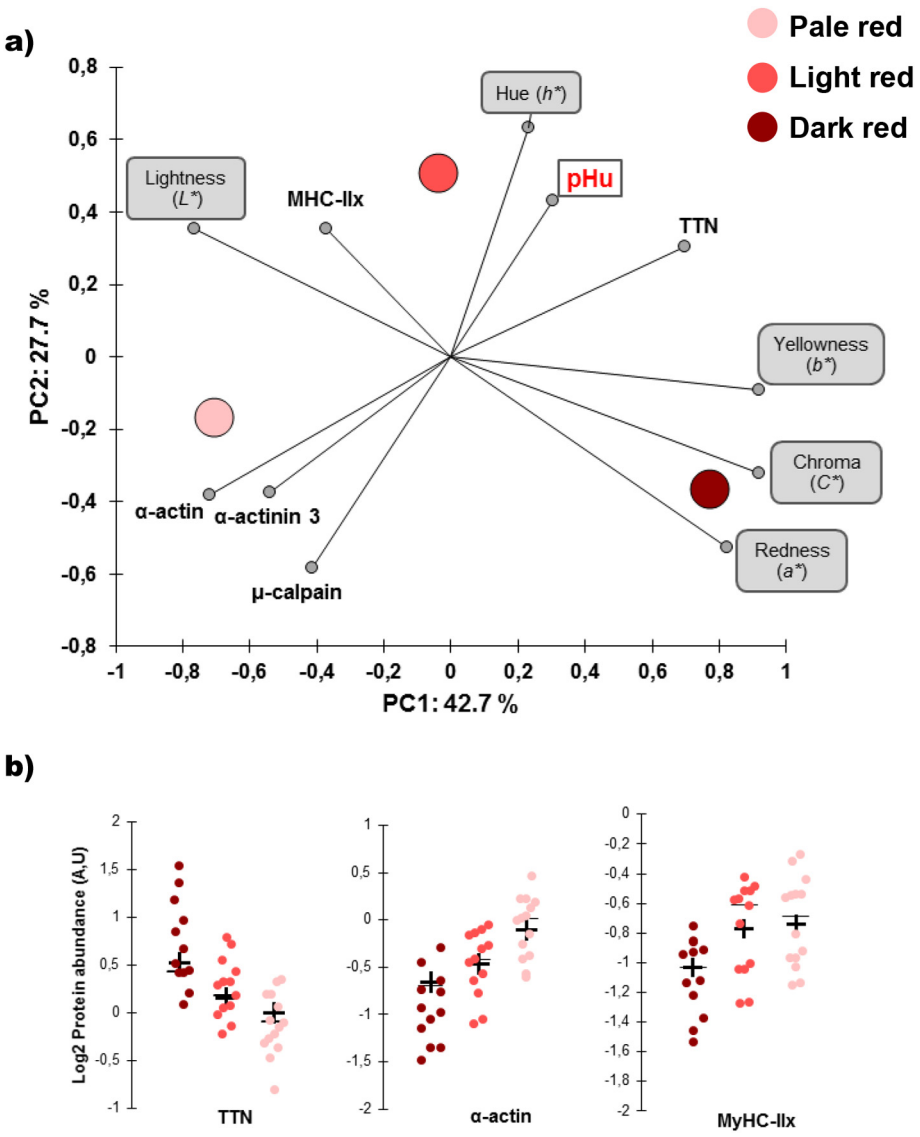

Fig. 5. Representation of the a) PCA using color coordinate parameters and differential proteins between the three meat color classes of *Longissimus thoracis* muscle of young Charolais bulls. The distribution of pale, light and dark red meat classes by their barycenters (centroids) are shown with circles using the corresponding schematic colors. The overall KMO was 0.76. b) Scatterplots of certain of the differential proteins (TTN, α-actin and MyHC-IIx) between the classes are shown to highlight the magnitude of differences and distribution of these biomarkers according to each class. (A colored version of the figure is available online).

biomarkers were also able to discriminate between muscle cuts color classes categorized according to their color characteristics. The study revealed that the relationships were in some cases color parameter-dependent and the variability explained in the regression equations is of great importance. This stresses that the mechanisms underlying meat color are complicated, and the use of high-throughput tools such as RPPA will be useful tools for making progress in the field. Notably, some previously unrelated proteins, like FHL1 and TRIM72, were for the first time identified to be associated with meat color. This study also revealed the complexity of the mechanisms that may be involved in meat color development. Overall, robust relationships were found between color and structural proteins, oxidative stress, heat stress and energy metabolism pathways. These pathways confirm once again that production-related traits in beef are the result of advanced biological processes finely orchestrated during the *p-m* muscle to meat conversion period.

Acknowledgements

The financial support given to Dr. Mohammed GAGAOUA from project S3-23000846 funded by Région Auvergne-Rhône-Alpes and FEDER is highly acknowledged. The authors acknowledge the financial support given by McKey Food Services, Valorex, and the Regional council of the French “Centre” for “Défiviande” project n°23000274. The authors are also grateful to Dr. Marie-Madeleine MIALON, the INRA coordinator of the project. Special thanks are addressed to Drs. Isabelle ORTIGUES-MARTY, Michel DOREAU and Didier MICOL from INRA-UMR1213 for their valuable expertise in the project management and help. The authors would thank the staff of INRA-UE232 (Bourges), INRA-UMR1213 (Theix) and INRA-UE 1414 Herbipôle (Theix) for animal care, management, slaughter and data collection. Many thanks to Nicole DUNOYER and Jeremey HUANT for their technical assistance in protein extractions for RPPA analyses. The authors thank also the Institut Curie RPPA platform for acquisition of RPPA data, namely Aurélie CARTIER and Bérengère OUINE. Finally, the authors are very grateful to Editor Dr. Michael DUGAN and to two anonymous referees for their valuable comments and suggestions on an earlier version of this manuscript.

Conflicts of interest

The authors declare that they have no conflict of interest.

Appendix A. Supplementary data

Supplementary data to this article can be found online at https://doi.org/10.1016/j.meatsci.2018.06.039.

References

Akbani, R., Becker, K. F., Carragher, N., Goldstein, T., de Koning, L., Korf, U., ... Zhu, J. (2014). Realizing the promise of reverse phase protein arrays for clinical, translational, and basic research: A workshop report: The RPPA (reverse phase protein Array) society. *Molecular & Cellular Proteomics, 13*(7), 1625–1643. https://doi.org/10.1074/mcp.O113.034918.

Almeida, A. M., Bassols, A., Bendixen, E., Bhide, M., Ceciliani, F., Cristobal, S., ... Turk, R. (2015). Animal board invited review: Advances in proteomics for animal and food sciences. *Animal, 9*(1), 1–17. https://doi.org/10.1017/S1751731114002602.

Bernard, C., Cassar-Malek, I., Le Cunff, M., Dubroeucq, H., Renand, G., & Hocquette, J. F. (2007). New indicators of beef sensory quality revealed by expression of specific genes. [research support, non-U S Gov't]. *Journal of Agricultural and Food Chemistry, 55*(13), 5229–5237. https://doi.org/10.1021/jf063372l.

Cai, C., Masumiya, H., Weisleder, N., Matsuda, N., Nishi, M., Hwang, M., ... Ma, J. (2009). MG53 nucleates assembly of cell membrane repair machinery. *Nature Cell Biology, 11*(1), 56–64. https://doi.org/10.1038/ncb1812.

Calnan, H., Jacob, R. H., Pethick, D. W., & Gardner, G. E. (2016). Production factors influence fresh lamb longissimus colour more than muscle traits such as myoglobin concentration and pH. *Meat Science, 119*(supplement C), 41–50. https://doi.org/10.1016/j.meatsci.2016.04.009.

Cassar-Malek, I., Guillemin, N., Hocquette, J. F., Micol, D., Bauchart, D., Picard, B., & Jurie, C. (2011). Expression of DNAJA1 in bovine muscles according to developmental age and management factors. *Animal, 5*(6), 867–874. https://doi.org/10.1017/S1751731110002491.

Chambaz, A., Scheeder, M. R. L., Kreuzer, M., & Dufey, P. A. (2003). Meat quality of Angus, Simmental, Charolais and Limousin steers compared at the same intramuscular fat content. *Meat Science, 63*(4), 491–500. https://doi.org/10.1016/s0309-1740(02)00109-2.

Chauhan, S. S., & England, E. M. (2018). Postmortem glycolysis and glycogenolysis: Insights from species comparisons. *Meat Science*. https://doi.org/10.1016/j.meatsci.2018.06.021.

Chaze, T., Hocquette, J.-F., Meunier, B., Renand, G., Jurie, C., Chambon, C., ... Picard, B. (2013). Biological markers for meat tenderness of the three main French beef breeds using 2-DE and MS approach. In F. Toldrá, & L. M. L. Nollet (Vol. Eds.), *Proteomics in foods. Vol. 2. Proteomics in foods* (pp. 127–146). USA: Springer.

Di Luca, A., Hamill, R. M., Mullen, A. M., Slavov, N., & Elia, G. (2016). Comparative proteomic profiling of divergent phenotypes for water holding capacity across the *post mortem* ageing period in porcine muscle exudate. *PLoS One, 11*(3), e0150605. https://doi.org/10.1371/journal.pone.0150605.

Duester, G. (2000). Families of retinoid dehydrogenases regulating vitamin a function. *European Journal of Biochemistry, 267*(14), 4315–4324. https://doi.org/10.1046/j.1432-1327.2000.01497.x.

Dunne, P. G., Keane, M. G., O'Mara, F. P., Monahan, F. J., & Moloney, A. P. (2004). Colour of subcutaneous adipose tissue and *M. longissimus* dorsi of high index dairy and beef × dairy cattle slaughtered at two liveweights as bulls and steers. *Meat Science, 68*(1), 97–106. https://doi.org/10.1016/j.meatsci.2004.02.010.

England, E. M., Matarneh, S. K., Scheffler, T. L., & Gerrard, D. E. (2017). Chapter 4 - Perimortal muscle metabolism and its effects on meat quality A2 - Purslow. In P. Peter (Ed.). *New aspects of meat quality* (pp. 63–89). Woodhead Publishing.

Farouk, M. M., Mustafa, N. M., Wu, G., & Krsinic, G. (2012). The "sponge effect" hypothesis: An alternative explanation of the improvement in the waterholding capacity of meat with ageing. *Meat Science, 90*(3), 670–677. https://doi.org/10.1016/j.meatsci.2011.10.012.

Franco, D., Mato, A., Salgado, F. J., Lopez-Pedrouso, M., Carrera, M., Bravo, S., ... Zapata, C. (2015). Tackling proteome changes in the longissimus thoracis bovine muscle in response to pre-slaughter stress. *Journal of Proteomics, 122*, 73–85. https://doi.org/10.1016/j.jprot.2015.03.029.

Fritz, J. D., & Greaser, M. L. (1991). Changes in titin and Nebulin in postmortem bovine muscle revealed by gel electrophoresis, western blotting and immunofluorescence microscopy. *Journal of Food Science, 56*(3), 607–610. https://doi.org/10.1111/j.1365-2621.1991.tb05340.x.

Funatsu, T., Kono, E., Higuchi, H., Kimura, S., Ishiwata, S., Yoshioka, T., ... Tsukita, S. (1993). Elastic filaments in situ in cardiac muscle: Deep-etch replica analysis in combination with selective removal of actin and myosin filaments. *The Journal of Cell Biology, 120*(3), 711–724.

Gagaoua, M., Bonnet, M., Ellies-Oury, M. P., De Koning, L., & Picard, B. (2018). Reverse phase protein arrays for the identification/validation of biomarkers of beef texture and their use for early classification of carcasses. *Food Chemistry, 250*(C), 245–252. https://doi.org/10.1016/j.foodchem.2018.01.070.

Gagaoua, M., Couvreur, S., Le Bec, G., Aminot, G., & Picard, B. (2017). Associations among protein biomarkers and pH and color traits in longissimus thoracis and rectus abdominis muscles in protected designation of origin Maine-Anjou cull cows. *Journal of Agricultural and Food Chemistry, 65*(17), 3569–3580. https://doi.org/10.1021/acs.jafc.7b00434.

Gagaoua, M., Hafid, K., Boudida, Y., Becila, S., Ouali, A., Picard, B., ... Sentandreu, M. A. (2015). Caspases and thrombin activity regulation by specific serpin inhibitors in bovine skeletal muscle. *Applied Biochemistry and Biotechnology, 177*(2), 279–303. https://doi.org/10.1007/s12010-015-1762-4.

Gagaoua, M., Monteils, V., Couvreur, S., & Picard, B. (2017). Identification of biomarkers associated with the rearing practices, carcass characteristics, and beef quality: An integrative approach. *Journal of Agricultural and Food Chemistry, 65*(37), 8264–8278. https://doi.org/10.1021/acs.jafc.7b03239.

Gagaoua, M., Picard, B., & Monteils, V. (2018). Associations among animal, carcass, muscle characteristics, and fresh meat color traits in Charolais cattle. *Meat Science, 140*, 145–156. https://doi.org/10.1016/j.meatsci.2018.03.004.

Gagaoua, M., Picard, B., Soulat, J., & Monteils, V. (2018). Clustering of sensory eating qualities of beef: Consistencies and differences within carcass, muscle, animal characteristics and rearing factors. *Livestock Science, 214*, 245–258. https://doi.org/10.1016/j.livsci.2018.06.011.

Gagaoua, M., Terlouw, E. M., Boudjellal, A., & Picard, B. (2015). Coherent correlation networks among protein biomarkers of beef tenderness: What they reveal. *Journal of Proteomics, 128*, 365–374. https://doi.org/10.1016/j.jprot.2015.08.022.

Gagaoua, M., Terlouw, E. M., Micol, D., Boudjellal, A., Hocquette, J. F., & Picard, B. (2015). Understanding early post-mortem biochemical processes underlying meat color and pH decline in the longissimus thoracis muscle of young blond d'Aquitaine bulls using protein biomarkers. *Journal of Agricultural and Food Chemistry, 63*(30), 6799–6809. https://doi.org/10.1021/acs.jafc.5b02615.

Gagaoua, M., Terlouw, E. M. C., Micol, D., Hocquette, J. F., Moloney, A. P., Nuernberg, K., ... Picard, B. (2016). Sensory quality of meat from eight different types of cattle in relation with their biochemical characteristics. *Journal of Integrative Agriculture, 15*(7), 1550–1563. https://doi.org/10.1016/s2095-3119(16)61340-0.

Gagaoua, M., Terlouw, E. M. C., Monteils, V., Couvreur, S., & Picard, B. (2017). Stress proteins in cull cows: relationships with transport and lairage durations but not with meat tenderness. *Paper presented at the proceedings of the 63rd international congress of meat science and technology, Cork, Ireland*.

Gagaoua, M., Terlouw, E. M. C., & Picard, B. (2017). The study of protein biomarkers to understand the biochemical processes underlying beef color development in young bulls. *Meat Science, 134*, 18–27. https://doi.org/10.1016/j.meatsci.2017.07.014.

Gao, X., Wu, W., Ma, C., Li, X., & Dai, R. (2015). Postmortem changes in sarcoplasmic proteins associated with color stability in lamb muscle analyzed by proteomics. *European Food Research and Technology, 242*(4), 527–535. https://doi.org/10.1007/s00217-015-2563-2.

Gardner, G. E., Hopkins, D. L., Greenwood, P. L., Cake, M. A., Boyce, M. D., & Pethick, D. W. (2007). Sheep genotype, age and muscle type affect the expression of metabolic enzyme markers. *Australian Journal of Experimental Agriculture, 47*(10), 1180–1189. https://doi.org/10.1071/EA07093.

Gatellier, P., Mercier, Y., Juin, H., & Renerre, M. (2005). Effect of finishing mode (pasture- or mixed-diet) on lipid composition, colour stability and lipid oxidation in meat from Charolais cattle. *Meat Science, 69*(1), 175–186. https://doi.org/10.1016/j.meatsci.2004.06.022.

Gregorio, C. C., Granzier, H., Sorimachi, H., & Labeit, S. (1999). Muscle assembly: A titanic achievement? *Current Opinion in Cell Biology, 11*(1), 18–25.

Huang, H., Larsen, M. R., Karlsson, A. H., Pomponio, L., Costa, L. N., & Lametsch, R. (2011). Gel-based phosphoproteomics analysis of sarcoplasmic proteins in post-mortem porcine muscle with pH decline rate and time differences. *Proteomics, 11*(20), 4063–4076. https://doi.org/10.1002/pmic.201100173.

Huff-Lonergan, E., & Lonergan, S. M. (2005). Mechanisms of water-holding capacity of meat: The role of postmortem biochemical and structural changes. *Meat Science, 71*(1), 194–204. https://doi.org/10.1016/j.meatsci.2005.04.022.

Huff-Lonergan, E., Zhang, W., & Lonergan, S. M. (2010). Biochemistry of postmortem muscle - lessons on mechanisms of meat tenderization. [review]. *Meat Science, 86*(1), 184–195. https://doi.org/10.1016/j.meatsci.2010.05.004.

Hughes, J., Clarke, F., Purslow, P., & Warner, R. (2017). High pH in beef longissimus thoracis reduces muscle fibre transverse shrinkage and light scattering which contributes to the dark colour. *Food Research International, 101*(Supplement C), 228–238. https://doi.org/10.1016/j.foodres.2017.09.003.

Hughes, J., Oiseth, S. K., Purslow, P. P., & Warner, R. D. (2014). A structural approach to understanding the interactions between colour, water-holding capacity and tenderness. *Meat Science, 98*(3), 520–532. https://doi.org/10.1016/j.meatsci.2014.05.022.

Hwang, I. H., Park, B. Y., Kim, J. H., Cho, S. H., & Lee, J. M. (2005). Assessment of postmortem proteolysis by gel-based proteome analysis and its relationship to meat quality traits in pig longissimus. *Meat Science, 69*(1), 79–91. https://doi.org/10.1016/j.meatsci.2004.06.019.

Jammes, Y., Steinberg, J. G., Delliaux, S., & Bregeon, F. (2009). Chronic fatigue syndrome combines increased exercise-induced oxidative stress and reduced cytokine and Hsp responses. *Journal of Internal Medicine, 266*(2), 196–206. https://doi.org/10.1111/j.1365-2796.2009.02079.x.

Jia, X., Hildrum, K. I., Westad, F., Kummen, E., Aass, L., & Hollung, K. (2006). Changes in enzymes associated with energy metabolism during the early post mortem period in longissimus thoracis bovine muscle analyzed by proteomics. *Journal of Proteome Research, 5*(7), 1763–1769. https://doi.org/10.1021/pr060119s.

Joseph, P., Suman, S. P., Rentfrow, G., Li, S., & Beach, C. M. (2012). Proteomics of muscle-specific beef color stability. *Journal of Agricultural and Food Chemistry, 60*(12), 3196–3203. https://doi.org/10.1021/jf204188v.

Jung, S. Y., & Ko, Y. G. (2010). TRIM72, a novel negative feedback regulator of myogenesis, is transcriptionally activated by the synergism of MyoD (or myogenin) and MEF2. *Biochemical and Biophysical Research Communications, 396*(2), 238–245. https://doi.org/10.1016/j.bbrc.2010.04.072.

Jurie, C., Martin, J.-F., Listrat, A., Jailler, R., Culioli, J., & Picard, B. (2005). Effects of age and breed of beef bulls on growth parameters, carcass and muscle characteristics. *Animal Science, 80*(03), 257–263. https://doi.org/10.1079/ASC40710257.

Kaiser, H. (1974). An index of factorial simplicity. *Psychometrika, 39*(1), 31–36. https://doi.org/10.1007/BF02291575.

Kwasiborski, A., Rocha, D., & Terlouw, C. (2009). Gene expression in large white or Duroc-sired female and castrated male pigs and relationships with pork quality. *Animal Genetics, 40*(6), 852–862. https://doi.org/10.1111/j.1365-2052.2009.01925.x.

Kwasiborski, A., Sayd, T., Chambon, C., Sante-Lhoutellier, V., Rocha, D., & Terlouw, C. (2008). Pig longissimus lumborum proteome: Part II: Relationships between protein content and meat quality. *Meat Science, 80*(4), 982–996.

Lange, S., Auerbach, D., McLoughlin, P., Perriard, E., Schafer, B. W., Perriard, J. C., & Ehler, E. (2002). Subcellular targeting of metabolic enzymes to titin in heart muscle may be mediated by DRAL/FHL-2. *Journal of Cell Science, 115*, 4925–4936 Pt 24.

Liu, Y., Lyon, B. G., Windham, W. R., Lyon, C. E., & Savage, E. M. (2004). Prediction of physical, color, and sensory characteristics of broiler breasts by visible/near infrared reflectance spectroscopy. *Poultry Science, 83*(8), 1467–1474.

Liu, Y., & Steinacker, J. M. (2001). Changes in skeletal muscle heat shock proteins: Pathological significance. *Frontiers in Bioscience, 6*(D12–25), D12–D25.

Lomiwes, D., Farouk, M. M., Frost, D. A., Dobbie, P. M., & Young, O. A. (2013). Small heat shock proteins and toughness in intermediate pHu beef. *Meat Science, 95*(3), 472–479. https://doi.org/10.1016/j.meatsci.2013.05.022.

Lomiwes, D., Farouk, M. M., Wu, G., & Young, O. A. (2014). The development of meat tenderness is likely to be compartmentalised by ultimate pH. *Meat Science, 96*(1), 646–651. https://doi.org/10.1016/j.meatsci.2013.08.022.

Matarneh, S. K., England, E. M., Scheffler, T. L., & Gerrard, D. E. (2017). Chapter 5 - the conversion of muscle to meat A2 - Toldra. *Fidel Lawrie's meat science* (pp. 159–185). (8th edn). Woodhead Publishing.

Mialon, M. M., Renand, G., Ortigues-Marty, I., Bauchart, D., Hocquette, J. F., Mounier, L., & Doreau, M. (2015). Fattening performance, metabolic indicators, and muscle composition of bulls fed fiber-rich versus starch-plus-lipid-rich concentrate diets1. *Journal of Animal Science, 93*(1), 319–333. https://doi.org/10.2527/jas.2014-7845.

Morzel, M., Chambon, C., Hamelin, M., Sante-Lhoutellier, V., Sayd, T., & Monin, G. (2004). Proteome changes during pork meat ageing following use of two different pre-slaughter handling procedures. *Meat Science, 67*(4), 689–696. https://doi.org/10.1016/j.meatsci.2004.01.008.

Morzel, M., Terlouw, C., Chambon, C., Micol, D., & Picard, B. (2008). Muscle proteome and meat eating qualities of longissimus thoracis of "blonde d'Aquitaine" young bulls: A central role of HSP27 isoforms [PFP - EXT]. *Meat Science, 78*(3), 297–304.

Nair, M. N., Suman, S. P., Chatli, M. K., Li, S., Joseph, P., Beach, C. M., & Rentfrow, G. (2016). Proteome basis for intramuscular variation in color stability of beef semimembranosus. *Meat Science, 113*, 9–16. https://doi.org/10.1016/j.meatsci.2015.11.003.

Nikoletopoulou, V., Markaki, M., Palikaras, K., & Tavernarakis, N. (2013). Crosstalk between apoptosis, necrosis and autophagy. *Biochimica et Biophysica Acta, 1833*(12), 3448–3459. https://doi.org/10.1016/j.bbamcr.2013.06.001.

Ohtsuka, H., Yajima, H., Maruyama, K., & Kimura, S. (1997). Binding of the N-terminal 63 kDa portion of connectin/titin to α-actinin as revealed by the yeast two-hybrid system. *FEBS Letters, 401*(1), 65–67. https://doi.org/10.1016/S0014-5793(96)01432-9.

Ouali, A., Gagaoua, M., Boudida, Y., Becila, S., Boudjellal, A., Herrera-Mendez, C. H., & Sentandreu, M. A. (2013). Biomarkers of meat tenderness: Present knowledge and perspectives in regards to our current understanding of the mechanisms involved. *Meat Science, 95*(4), 854–870. https://doi.org/10.1016/j.meatsci.2013.05.010.

Papa, I., Astier, C., Kwiatek, O., Raynaud, F., Bonnal, C., Lebart, M.-C., & Benyamin, Y. (1999). Alpha actinin–CapZ, an anchoring complex for thin filaments in Z-line. *Journal of Muscle Research & Cell Motility, 20*(2), 187–197. https://doi.org/10.1023/A:1005489319058.

Paweletz, C. P., Charboneau, L., Bichsel, V. E., Simone, N. L., Chen, T., Gillespie, J. W., & Liotta, L. A. (2001). Reverse phase protein microarrays which capture disease progression show activation of pro-survival pathways at the cancer invasion front. *Oncogene, 20*(16), 1981–1989. https://doi.org/10.1038/sj.onc.1204265.

Picard, B., & Gagaoua, M. (2017). Chapter 11 - proteomic investigations of beef tenderness. *Proteomics in food science: From farm to fork* (pp. 177–197). Academic Press.

Picard, B., Gagaoua, M., Al-Jammas, M., De Koning, L., Valais, A., & Bonnet, M. (2018). Beef tenderness and intramuscular fat proteomic biomarkers: Muscle type effect. *Peer Journal, 6*, e4891. https://doi.org/10.7717/peerj.4891.

Picard, B., Gagaoua, M., & Hollung, K. (2017). Chapter 12 - gene and Protein expression as a tool to explain/predict meat (and fish) quality. *New aspects of meat quality: From genes to ethics* (pp. 321–354). Woodhead Publishing.

Picard, B., Gagaoua, M., Micol, D., Cassar-Malek, I., Hocquette, J. F., & Terlouw, C. E. (2014). Inverse relationships between biomarkers and beef tenderness according to contractile and metabolic properties of the muscle. *Journal of Agricultural and Food Chemistry, 62*(40), 9808–9818. https://doi.org/10.1021/jf501528s.

Polati, R., Menini, M., Robotti, E., Millioni, R., Marengo, E., Novelli, E., & Cecconi, D. (2012). Proteomic changes involved in tenderization of bovine longissimus dorsi muscle during prolonged ageing. *Food Chemistry, 135*(3), 2052–2069. https://doi.org/10.1016/j.foodchem.2012.06.093.

Priolo, A., Micol, D., & Agabriel, J. (2001). Effects of grass feeding systems on ruminant meat colour and flavour. A review. *Animal Research, 50*(3), 185–200.

Pulford, D. J., Dobbie, P., Fraga Vazquez, S., Fraser-Smith, E., Frost, D. A., & Morris, C. A. (2009). Variation in bull beef quality due to ultimate muscle pH is correlated to endopeptidase and small heat shock protein levels. *Meat Science, 83*(1), 1–9. https://doi.org/10.1016/j.meatsci.2008.11.008.

Raynaud, F., Bonnal, C., Fernandez, E., Bremaud, L., Cerutti, M., Lebart, M.-C., & Benyamin, Y. (2003). The calpain 1–α-actinin interaction. *European Journal of Biochemistry, 270*(23), 4662–4670. https://doi.org/10.1046/j.1432-1033.2003.03859.x.

Renerre, M. (1990). Factors involved in the discoloration of beef meat. *International Journal of Food Science & Technology, 25*(6), 613–630. https://doi.org/10.1111/j.1365-2621.1990.tb01123.x.

Sedoris, K. C., Thomas, S. D., & Miller, D. M. (2010). Hypoxia induces differential translation of enolase/MBP-1. *BMC Cancer, 10*, 157. https://doi.org/10.1186/1471-2407-10-157.

Shathasivam, T., Kislinger, T., & Gramolini, A. O. (2010). Genes, proteins and complexes: The multifaceted nature of FHL family proteins in diverse tissues. *Journal of Cellular and Molecular Medicine, 14*(12), 2702–2720. https://doi.org/10.1111/j.1582-4934.2010.01176.x.

Taylor, R. G., Geesink, G. H., Thompson, V. F., Koohmaraie, M., & Goll, D. E. (1995). Is Z-disk degradation responsible for postmortem tenderization? *Journal of Animal Science, 73*(5), 1351–1367.

Troncale, S., Barbet, A., Coulibaly, L., Henry, E., He, B., Barillot, E., & de Koning, L. (2012). NormaCurve: A SuperCurve-based method that simultaneously quantifies and normalizes reverse phase protein array data. *PLoS One, 7*(6), e38686. https://doi.org/10.1371/journal.pone.0038686.

Vasiliou, V., Thompson, D. C., Smith, C., Fujita, M., & Chen, Y. (2012). Aldehyde dehydrogenases: From eye crystallins to metabolic disease and cancer stem cells. *Chemico-Biological Interactions, 16*(12), 00233–00235. https://doi.org/10.1016/j.cbi.2012.10.026.

Wu, W., Gao, X. G., Dai, Y., Fu, Y., Li, X. M., & Dai, R. T. (2015). Post-mortem changes in sarcoplasmic proteome and its relationship to meat color traits in M. Semitendinosus of Chinese Luxi yellow cattle. *Food Research International, 72*(0), 98–105. https://doi.org/10.1016/j.foodres.2015.03.030.

Wu, W., Yu, Q. Q., Fu, Y., Tian, X. J., Jia, F., Li, X. M., & Dai, R. T. (2016). Towards muscle-specific meat color stability of Chinese Luxi yellow cattle: A proteomic insight into post-mortem storage. *Journal of Proteomics, 147*, 108–118. https://doi.org/10.1016/j.jprot.2015.10.027.

Yu, Q., Wu, W., Tian, X., Hou, M., Dai, R., & Li, X. (2017). Unraveling proteome changes of Holstein beef M. Semitendinosus and its relationship to meat discoloration during post-mortem storage analyzed by label-free mass spectrometry. *Journal of Proteomics, 154*, 85–93. https://doi.org/10.1016/j.jprot.2016.12.012.